Investigation of Low Temperature Cracking in Asphalt Pavements

National Pooled Fund Study – Phase II

Task 3- Develop Low Temperature Specification for Asphalt Mixtures

Subtask 3- *Development of the Single-Edge Notched Beam (SENB) Test*

Hassan A. Tabatabaee
Raul Velasquez
Sebastian Puchalski
Hussain U. Bahia

University of Wisconsin-Madison

January 2012

TABLE OF CONTENTS

LIST OF FIGURES

LIST OF TABLES

Introduction

It is recognized that a better approach for thermal cracking characterization of asphalt materials is to use fracture mechanics principles rather than to use continuum mechanics approach of linear viscoelastic materials. Current test methods to address low temperature cracking, such as the Bending Beam Rheometer (BBR) (1), characterize the material in the linear viscoelastic domain at small strain levels and, therefore, do not provide the complete picture for thermal cracking characterization.

Previous research by Hoare and Hesp (2), Hesp (3), Chailleux and Mouillet (4), Chailleux et al. (5) have used the Single-Edge Notched Bending (SENB) Test, which is a fracture mechanics-based test commonly used in metals and other materials, to obtain the fracture properties of asphalt binders at low temperatures. They succeeded in grading a broad range of materials with different levels of modification. The SENB test follows ASTM E399 standard (6) and assumes that linear elastic fracture mechanics (LEFM) conditions hold. Figure 1 shows a schematic of how the SENB test is performed and the parameters used for the calculation of fracture toughness (K_{IC}) and fracture energy (G_f).

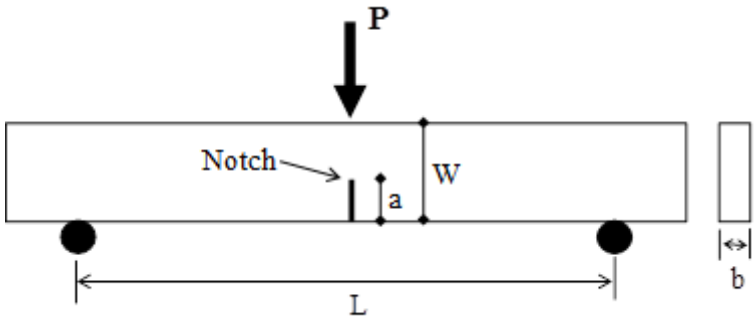

Figure 1. SENB test schematic.

The following equation is used to calculate the fracture toughness, K_{IC}, of asphalt binders:

$$K_{IC} = \frac{PL}{bW^{3/2}} f\left(\frac{a}{W}\right) \tag{1}$$

with $f\left(\frac{a}{W}\right)$ defined for SENB geometry as:

$$f\left(\frac{a}{W}\right) = \frac{3\left(\frac{a}{W}\right)^{\frac{1}{2}}\left[1.99 - \frac{a}{W}\left(1-\frac{a}{W}\right)\left(2.15 - 3.93\left(\frac{a}{W}\right) + 2.7\left(\frac{a}{W}\right)^2\right)\right]}{2\left(1+2\frac{a}{W}\right)\left(1-\frac{a}{W}\right)^{\frac{3}{2}}} \tag{2}$$

The K_{IC} parameter denotes mode I fracture in which crack formation occurs in tensile mode due to bending.

The fracture energy, G_f is calculated as the total area under the entire load-deflection (P-u) curve, divided by the area of the ligament. This is shown in equation (3).

$$G_f = \frac{W_f}{A_{lig}} \quad (3)$$

where:

- $W_f = \int Pdu$,
- And A_{lig} is the area of the ligament.

The commonly used SENB specimen geometry proposed in recent studies (2-5) includes two metal bars to reduce the amount of asphalt binder used. However, when this geometry was used in testing, adhesion problems between the asphalt binder and the metal bars observed during sample preparation and handling of the specimen motivated the use of a new geometry based on the BBR specimens, without the need for the metal bars. The new proposed geometry can be used in the SENB system for low temperature characterization and ranking of a broad range of unmodified and modified asphalt binders.

The Single Edged Notched Beam Test

Proposed SENB Geometry

A new SENB geometry that adds a notch to the beams made using common BBR molds has been introduced. The new geometry resolves the adhesion problem encountered (Figure 2) by eliminating the need for metal bars and simplifying the specimen preparation procedure (7). It is noted that the sample preparation procedure is less time consuming and simpler when using the proposed BBR sample molds with minor modification to allow for inserting the notch.

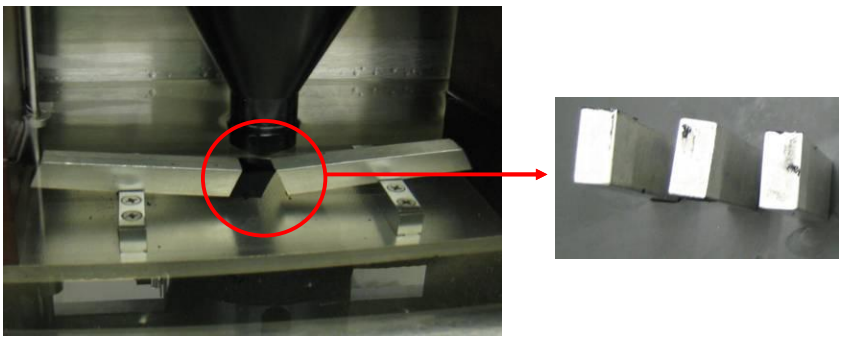

Figure 2. Adhesion problems observed in current SENB geometry.

The proposed notched BBR beams can be prepared by making a notch of 3 mm (i.e., corresponding to 20-25% of beam depth, similar to previous geometry) in the wide side (i.e., 12.7 mm) of the BBR mold side-beams. The mold can still be used for regular BBR beam fabrication as the notch is very thin and can be covered with the plastic sheets commonly used in BBR molding (Figure 3).

Figure 2. SENB specimen mold.

Note that the height to width proportions of the existing SENB geometry and the BBR beams remain unchanged. The new geometry scales the dimensions by ½. This geometry uses the same amount of asphalt binder (i.e., 10 g) required in the BBR standard and the current SENB composite beams, while resolving the adhesion problem between the binder and the metal bars.

Finite Element Simulations

Finite element (FE) simulations of both geometries were performed using the ABAQUS software package (8) to investigate differences between stress distributions around the notch from both geometries and to determine stress discontinuities in the current geometry.

For the FE simulations, the asphalt binder was considered as a linear viscoelastic material with G_0 = 3 GPa, ν = 0.3, and the Prony series coefficients shown in Table 1. For the metal bars, an elastic material with G_0 = 70 GPa and ν = 0.3 was used. The FE simulations were performed with standard 3D stress quadratic elements with reduced integration. The simulations were divided into two steps. First, the beam was loaded with a rate of 0.01 mm/sec for 1 sec, then a constant displacement of 0.01 mm was maintained for a period of 100 sec.

Table 1. Prony series coefficients for FE simulations.

G_i	K_i	τ_i
0.12	0.12	2.89
0.07	0.07	33.01
0.08	0.08	334.09

Figure 4 shows the results from the FE simulations for both geometries. The finite element simulations indicate that the stress distributions around the notch for both geometries are very similar. Furthermore, the current SENB composite geometry shows stress discontinuity at the interface between the metal bars and the asphalt binder (Figure 4(b)), which may have a significant effect on the results of the test. Use of the standard BBR geometry results in uniform stress field outside of the loading and notch area, as showing in Figure 4(a).

(a) Proposed BBR Geometry

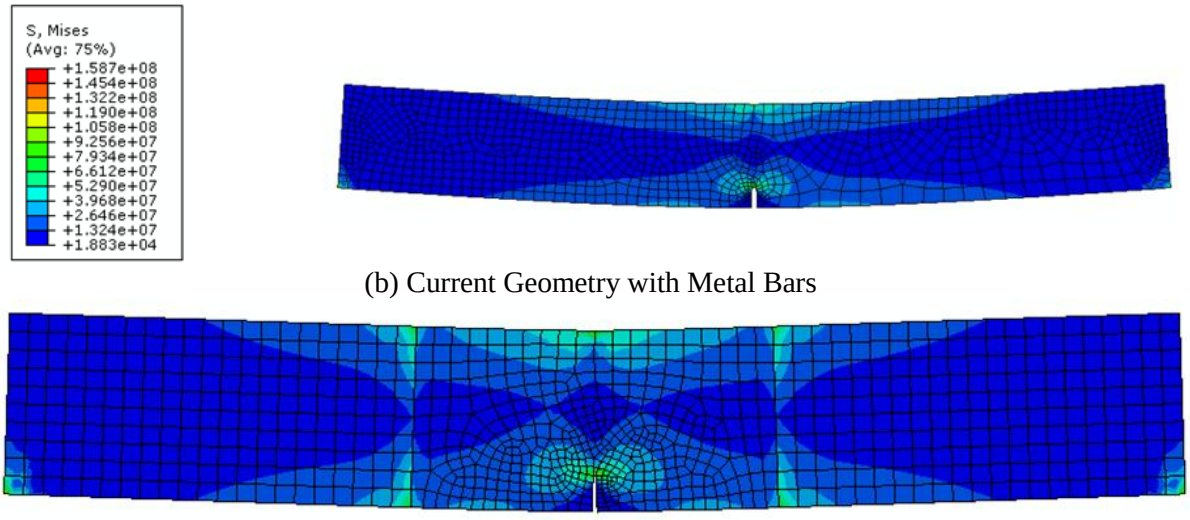

(b) Current Geometry with Metal Bars

Figure 4. Stress distribution for (a) proposed and (b) current SENB geometry from Finite Element simulations.

Single-Edge Notched Bending (SENB) Test Procedure

The BBR-SENB system which is very similar to current BBR is shown in Figure 5. The difference between the systems is in the addition of a loading motor that controls the displacement rate during testing and also in using a load cell with a higher load capacity than the regular BBR. Each test is run at a constant displacement rate of 0.01 mm/sec.

Figure 5. SENB system.

Fracture properties of asphalt binders can be derived from failure tests on notched samples. These properties are of interest as they are measured at high strain values compared to the BBR, thus damage characterization is taken into account, which is especially important for modified asphalt binders.

The fracture parameters investigated included the load and displacement at fracture, the fracture toughness, K_{IC}, and the fracture energy (G_f). The fracture load was determined to be the peak load occurring during the test, and the fracture deformation was the

corresponding deformation at the peak load. Depending on the binder type and test temperature, failure can occur at the peak load or at a lower load after the peak.

The European standard CEN/TS 15963:2010 "Bitumen and bituminous binders - Determination of the fracture toughness temperature by a three point bending test on a notched specimen," specifies another fracture parameter referred to as the "Fracture Temperature" or T_{FT} (9). This parameter is the lowest temperature at which the displacement at the maximum load is 0.3 mm. It is speculated that this displacement value can be used as threshold to determine ductile to brittle transition of asphalt binders. To determine this point, the deflections at maximum load at different test temperatures are fitted with an exponential curve as shown in Figure 6.

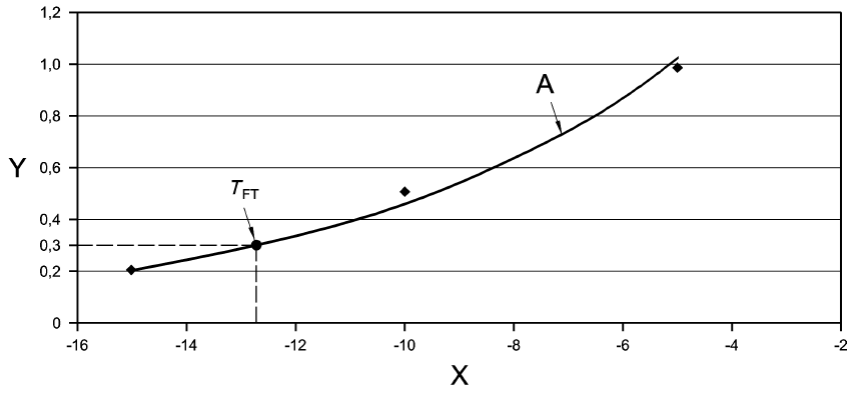

Figure 6. Temperature (X in °C) vs. Deflection at Maximum Load Curve (Y in mm) (9).

Sources of variability in SENB

The sources of variability were identified and minimized. The repeatability of the test results was significantly improved after addressing the following issues:

- Damage to the sample notch during the de-molding process.
- Improper alignment of the loading shaft and the sample notch during loading.
- Variation in load calibration constants from test to test.

Although these factors varied in their relative effect on variability, all were deemed important. The following preventive actions were implemented in the SENB test procedure:

- Adding alignment pins to the aluminum mold setup (Figure 7) to prevent the movement of the mold end pieces relative to the notch position, which could potentially result in off center or angled notches on the sample beam.
- Recording the load calibration factor generated for every replicate and scaling all the results for a set of replicates to an average consistent calibration factor. This action is deemed a temporary solution. Efforts are being made to modify the test software to correct this issue.
- Specific control of the de-molding process to ensure minimal stress application to notch.
- Refrigeration of samples before de-molding to prevent excessive deformation during handling.

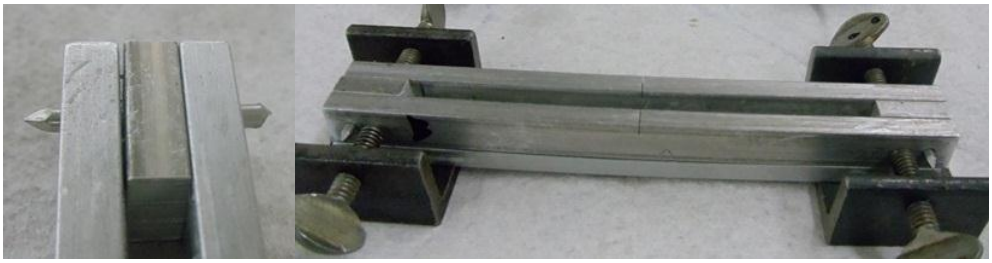

Figure 7. Modified SENB mold system with alignment pins.

Figure 8 shows an example of SENB replicates after implementing aforementioned improvements to reduce variability. Test results showed the effectiveness of the mold alignment pins in limiting variability in fracture deflection, as well as the effect of the calibration factor correction in minimizing variability in the fracture load. Results of test sets ran after these changes show highly repeatable replicates with COV of fracture load and deformation generally under 10%.

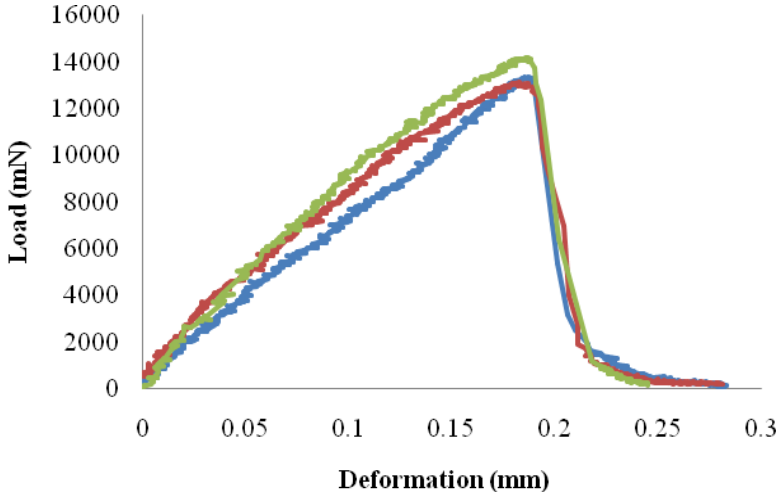

Figure 8. Results of SENB replicates after procedure improvement.

Materials

The seven binders described in Task 2 were tested using the BBR-SENB, BBR, glass transition temperature test, and the Asphalt Binder Cracking Device (ABCD). Table 2 presents a description of these binders. All binders were subjected to short-term aging using the Rolling Thin Film Oven (RTFO). Furthermore, a large set of modified and unmodified binders from the Asphalt Research Consortium project, as well as binders from select LTPP validation sections were included in the test matrix. Details on how the glass transition temperature and ABCD tests were performed can be found in (7).

Table 2. Description of the Asphalt Binders Tested in BBR-SENB.

Binder	Location	Description
PG 58-34 PPA	MnROAD 33	Modified with Polyphosphoric Acid (PPA)
PG 58-34 SBS+PPA	MnROAD 34	Modified with Styrene-Butadiene Styrene (SBS) +PPA
PG 58-34 SBS	MnROAD 35	Modified with SBS
PG 58-34 Elvaloy +Acid	MnROAD 77	Modified with PPA + Elvaloy
PG 58-28	MnROAD 20	Neat
PG 58-34	MnROAD 22	Unknown Modification
PG 64-22	Wisconsin	Binder used in construction of SMA pavement in Wisconsin

Results and Discussion

SENB vs. BBR

BBR-SENB and BBR measurements were compared for an extensive set of binders which included materials in Table 2 and binders used in the Asphalt Research Consortium (ARC). In these tests the S(60) and m-value of the asphalt binders were measured after 1 hr of conditioning at the same temperatures used for the BBR-SENB testing.

Although no specification for determining pavement performance based on low temperature fracture parameters exists, intuitively one would expect higher K_{IC} and G_f to indicate better performance.

The SENB parameters (i.e., G_f and K_{IC}) are plotted against the m-value and S(60) in Figures 9 and 10, respectively. It should be noted that all correlations made in subsequent sections are meant to compare the ranking capability of different low temperature performance indices and are not for the purpose of deriving direct relationships between the indices.

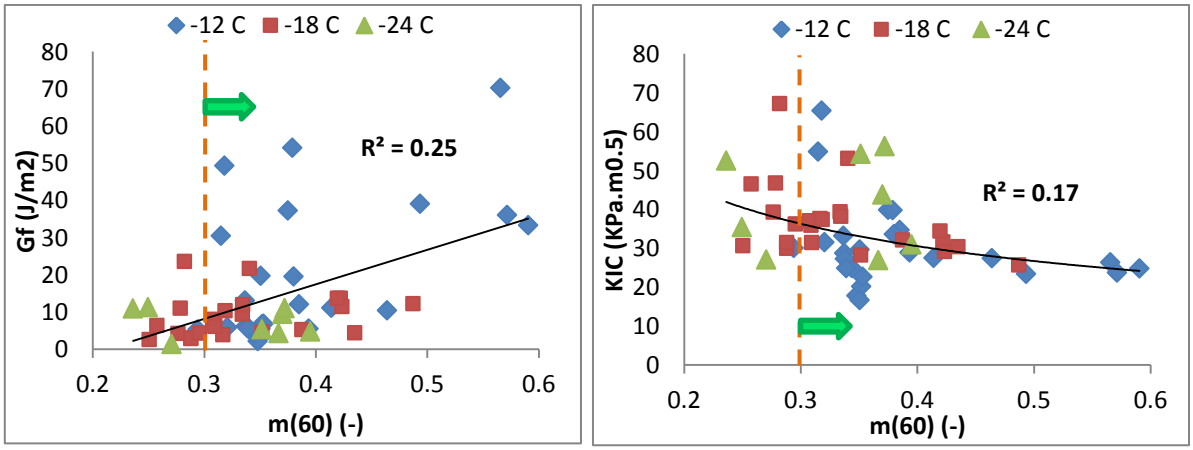

Figure 9. SENB G_f and K_{IC} plotted against BBR m-value at different temperatures (Hatched line show Superpave BBR criteria limit; green arrow shows side passing this criterion).

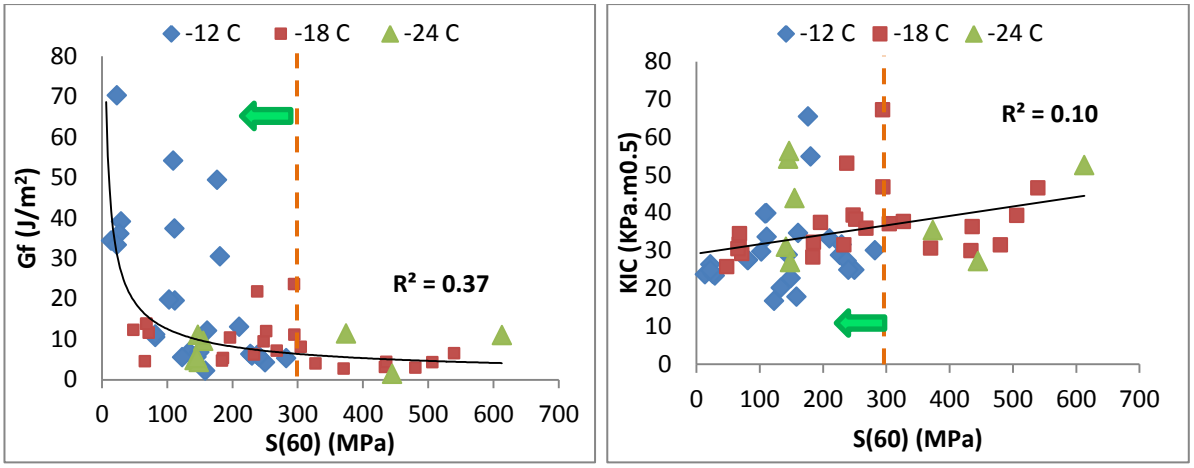

Figure 10. SENB G_f and K_{IC} plotted against BBR creep stiffness at different temperatures (Hatched line show Superpave BBR criteria limit; green arrow shows side passing this criterion)

The trends in Figures 9 and 10 show that the m-value (m(60)) and creep stiffness (S(60)) have very poor correlation with the fracture parameters obtained in the SENB test. It can also be seen that the BBR m-value and creep stiffness limits fail to account for many binders demonstrating poor fracture performance in terms of fracture energy. Furthermore, the SENB fracture energy (G_f) clearly discriminates between binders with similar stiffness and m-value, especially for the range passing the Superpave criteria (S< 300 MPa, and m> 0.300), indicating its potential as a performance index.

SENB vs. T_g

The glass transition temperature (T_g) is related to the asphalt binder performance at low temperatures. The transition to glassy behavior is known to increase the brittleness of the binder extensively, reducing the potential for stress relaxation, increasing stiffness, and thus resulting in higher cracking susceptibility.

The fracture energy from the SENB test at -12°C is compared to the glass transition temperature in Figure 11. It is observed that these parameters are closely related. The lower the glass transition temperature is, the lower the brittleness of the asphalt binder, and thus higher deformation to failure is expected. As the observed variation in peak fracture load was relatively low for different binders, the fracture deformation is usually the controlling parameter in the fracture energy. This leads to higher fracture energy for asphalt binders with lower glass transition temperatures and consequently higher ductility. Asphalt binders with low T_g are believed to have superior crack resistance in comparison to binders with higher T_g. This relationship is shown in Figure 11, using BBR-SENB data at -12°C.

The correlations between T_g and BBR parameters shown in Figure 12 are lower than the correlations observed between T_g and BBR-SENB fracture parameters. Note that the BBR measures properties in relatively small strains in the linear viscoelastic region in comparison to the BBR-SENB fracture parameters, which are measured at large strains.

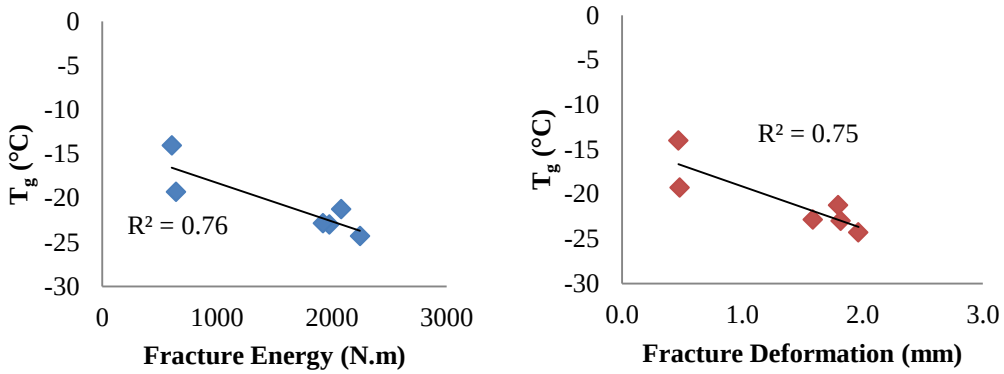

Figure 3. Glass transition temperature plotted against the BBR-SENB fracture Energy and fracture deformation at -12°C.

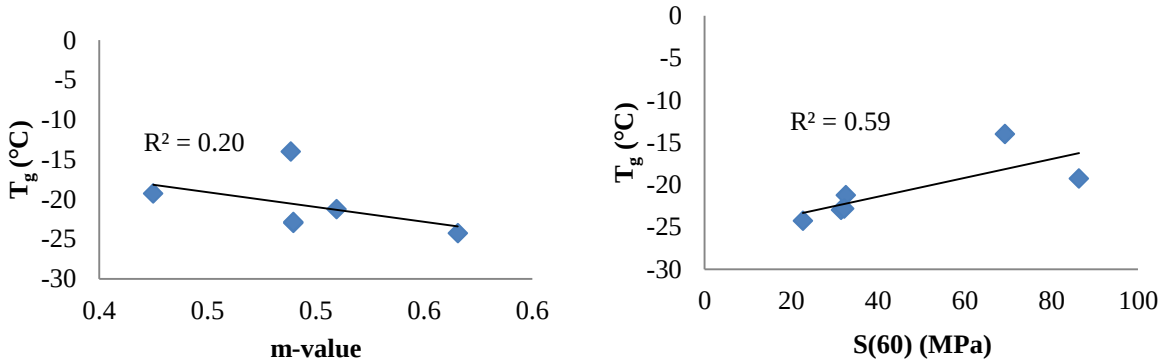

Figure 4. T_g plotted against BBR parameters at -12°C.

SENB vs. ABCD

The Asphalt Binder Cracking Device (ABCD) has recently been introduced as another test method for determining the low temperature performance of binders (11). This test was used to investigate thermal cracking susceptibility of the asphalt binders. An important observation from the ABCD results was that the average critical cracking temperature determined from the tested binders (i.e., approximately -40°C) is about 20°C lower than the other low temperature indices measured (e.g., average T_g and average T_{FT} are both approximately -20°C). The ABCD critical cracking temperatures were compared to parameters from the BBR, SENB and T_g tests. These correlations are presented in Figures 13, 14, and 15.

Figure 13 shows the T_{FT} parameter from the SENB and the glass transition temperature (T_g) plotted against the ABCD cracking temperature. As expected the trend for both T_{FT} and T_g are almost identical. This is not surprising considering the equivalency established between these two parameters. In either case, there is a poor correlation between the ABCD cracking temperature and the T_{FT} and T_g.

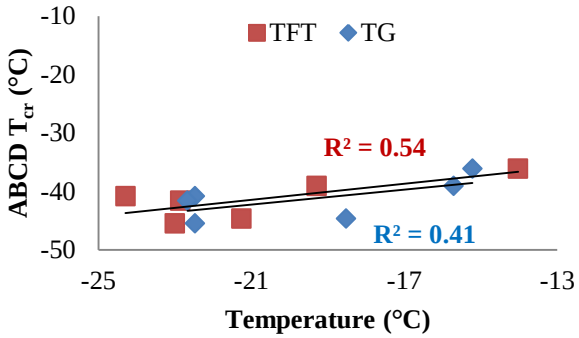

Figure 13. ABCD critical cracking temperature plotted against T_{FT} and T_g.

Figures 14 and 15 show that the SENB fracture load and deformation have a moderate correlation with the ABCD results. On the other hand, the correlation between the ABCD cracking temperature and the BBR parameters, especially the m-value, is relatively poor. It is recognized that the ABCD and the BBR-SENB are fundamentally different tests, since the first uses a thermally restrained sample with a circular hole while the second uses an unrestrained sample with a sharp notch to initiate crack propagation. It is not clear at this time which of these measures gives the best prediction of pavement cracking.

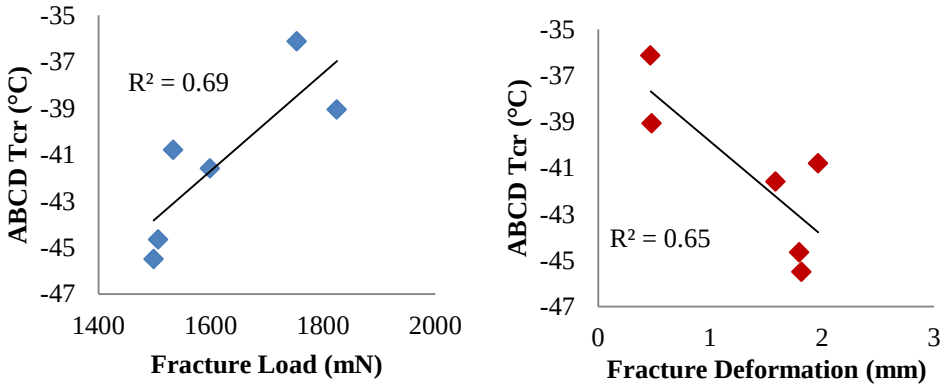

Figure 14. ABCD critical cracking temperature plotted against SENB fracture load and deformation.

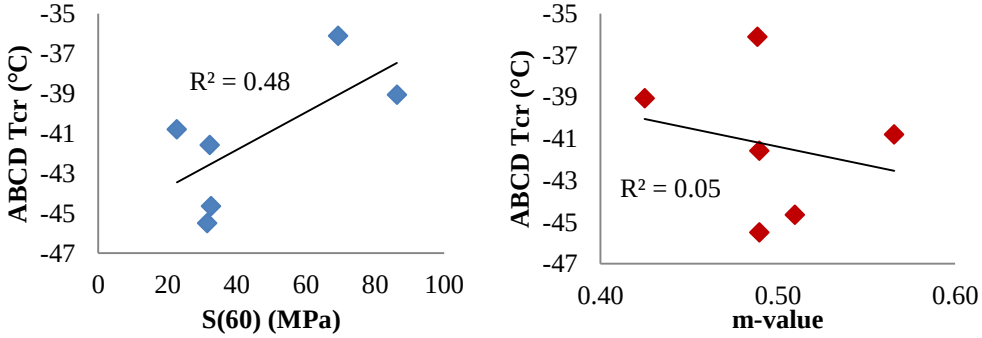

Figure 15. ABCD critical cracking temperature plotted against BBR parameters.

Effect of Physical Hardening on SENB Fracture Properties

The effect of isothermal conditioning on binder fracture properties was also investigated. Figure 16 depicts results of testing five binders from Table 2 after 0.5 and 72 hr of conditioning at their glass transition temperature (T_g). A 37% average increase in stiffness was observed, as indicated by the slope of the P-u curve after conditioning. The fracture toughness also increased for all binder tested after conditioning; however, the effect on fracture energy was not clear. Fracture energy increased for the 2 unmodified binders (i.e., MnROAD Cell 20 and NY), while decreasing for the 3 modified binders. This reduction is explained by the relative loss of strain tolerance with conditioning time. In other words, the increase in load at fracture is offset by reduction in deformation at break for the unmodified binders. The observed trend is more clearly shown for each parameter in Figure 17, in which results are normalized to their respective values measured after 0.5 hr of isothermal conditioning.

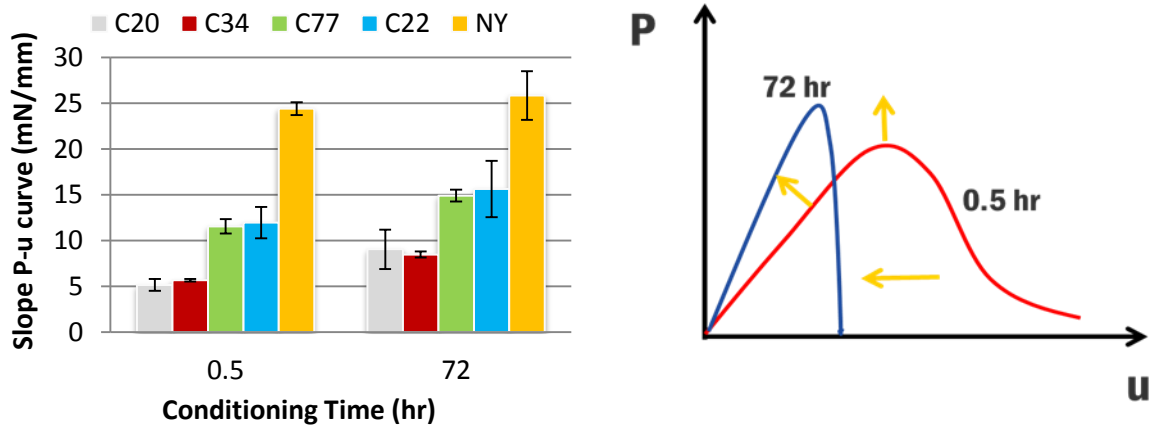

(a) **(b)**

Figure 16. (a) Slope of P-u curve before and after isothermal conditioning at T_g. (b) Schematic of general trend observed after conditioning.

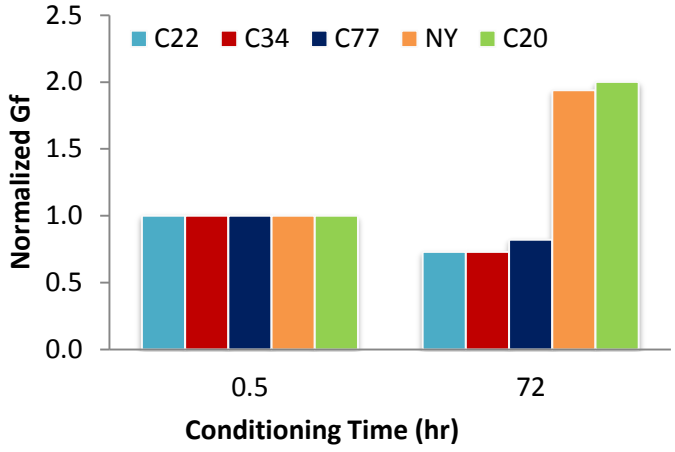

(a)

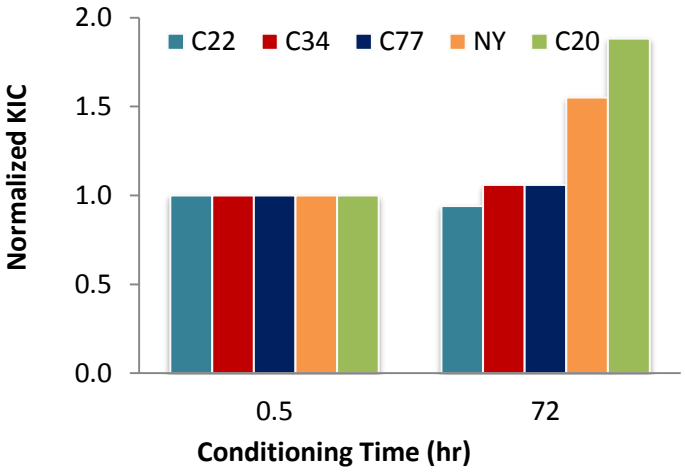

(b)

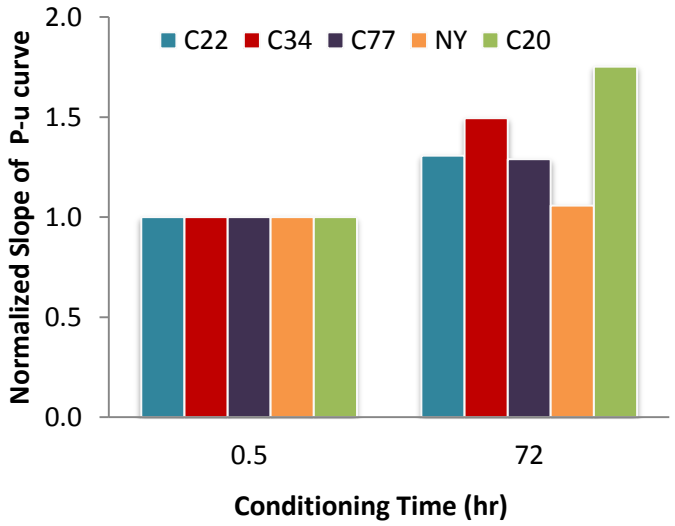

(c)

Figure 17. Normalized SENB parameters (a) G_f, (b) K_{IC}, and (c) slope of P-u curve, after 0.5 and 72 hrs of conditioning.

SENB as a Low Temperature Performance Specification

As part of the SHRP research project, the Bending Beam Rheometer (BBR) and the Direct Tension Test (DTT) were introduced as methods to characterize the low temperature performance of asphalt binders.

The BBR used creep stiffness (S(t)) and a relaxation related parameter designated as the m-value, to characterize binders at low temperatures. These parameters were measured under a relatively small load and a short loading time, thus the experienced strain levels were relatively low, resulting in most binders performing in the linear viscoelastic range. Based on the nature of the thermal cracking distress, a fracture test method would seem to be the most direct method of simulating this phenomenon in a laboratory environment. Early studies have introduced the DTT test to measure brittleness and strain tolerance, but the test was shown to be hardly repeatable and very difficult to conduct. Early studies showed that the low temperature failure strain at break is highly correlated with the binder stiffness for unmodified binders (14, 15). However, these studies did not take into account the effect of modification. Non-linearity combined with damage propagation in the binder can significantly complicate the behavior of modified asphalt binders at large strains. This has inspired some researchers to develop specifications that predict the binder's critical cracking temperature using calculations based on DTT and BBR results and fundamental mechanics modeling (14, 15).

The DTT applied a tensile load on the binder until failure occurred, reporting the failure stress and strain. As with many fracture tests, numerous complications in sample preparation and repeatability, have ultimately led to the exclusion of this test as part of the specification.

In this study the BBR-SENB test was evaluated as a possible alternative to the DTT test for estimation of strain tolerance, as well as providing valuable information on binder fracture resistance. The BBR-SENB is able to capture the ductile-brittle transition of binders and differentiate between fracture performances of binders of the same BBR low temperature performance grade. Figure 18 shows the difference in performance as measured by the SENB for binders of the same PG tested at -12°C, and -24°C. The binders tested correspond to a wide range of modified and unmodified binders presented in Table 2, binders obtained from WRI verification sections (Task 6), and LTPP sections.

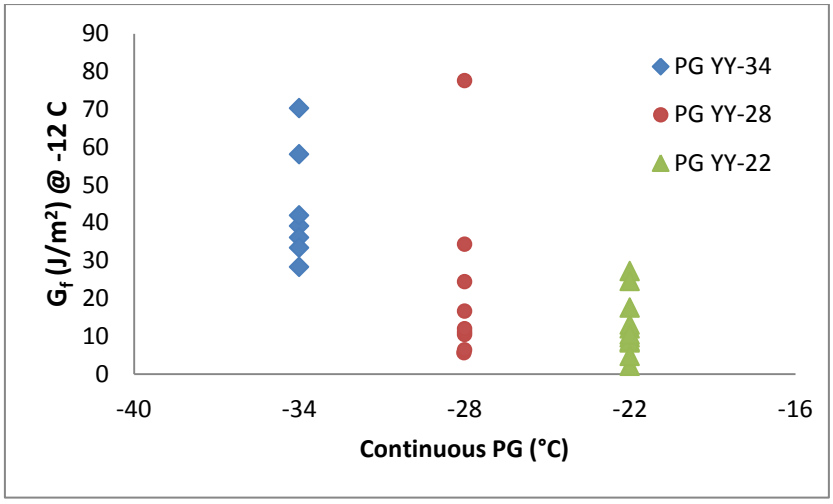

(a)

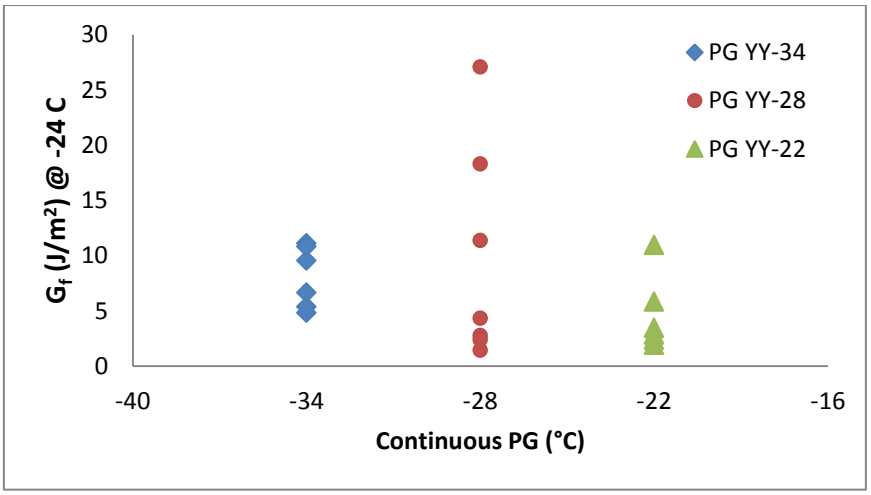

(b)

Figure 18. Difference in performance as measured by the SENB G_f for binders of the same PG, tested at (a) -12°C, and (b) -24°C.

Figure 18 clearly shows a great difference in fracture energy for binders classified as the same performance grade using the Superpave BBR specification. It can be seen that binders that perform similarly based on the creep stiffness and m-value, can show up to 10 times difference in fracture energy. These results demonstrate the ability of the SENB fracture energy (G_f) to differentiate between different modified and unmodified binder systems in terms of low temperature performance.

Another important factor investigated in the BBR-SENB, was the ability to capture the brittle-ductile transition behavior of binders (assumed to be due to material undergoing glass transition) at low temperatures. SENB results in terms of fracture energy (G_f), fracture toughness (K_{IC}) and fracture deformation were plotted based on the relative distance of the test temperature to the respective binder's glass transition temperature (Figure 19). The T_g measurements were obtained using a dilatometric system described in (7) and included as part of the experimental plan in Task 5.

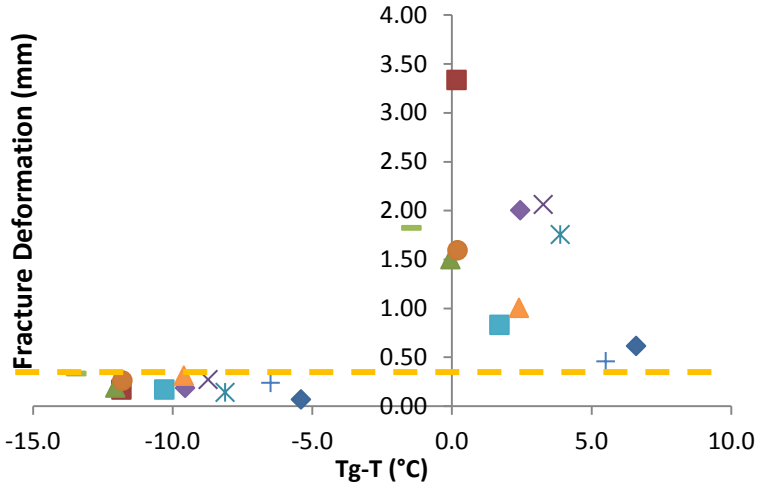

(a)

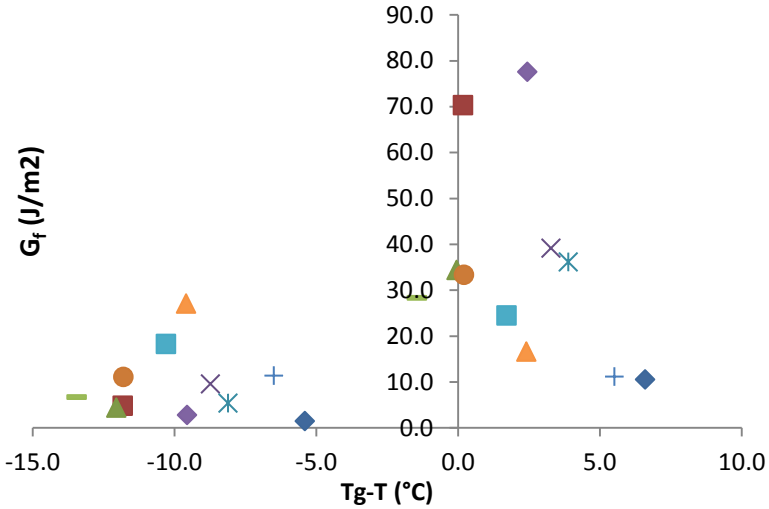

(b)

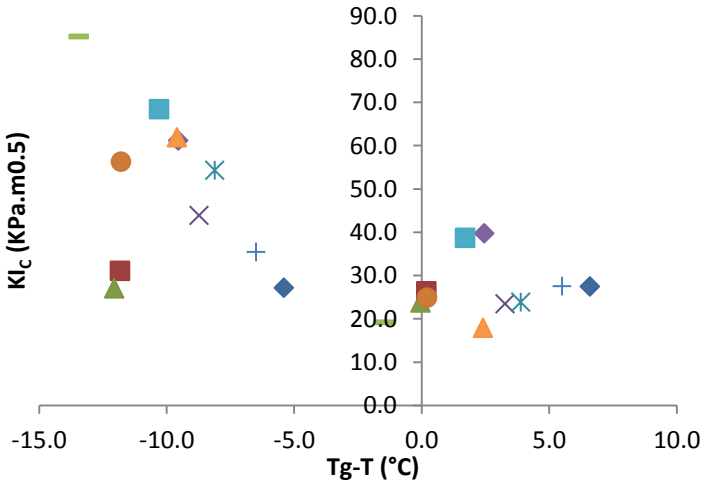

(c)

Figure 19. Brittle-ductile transition behavior using SENB parameters (a) Fracture deflection, (b) Fracture energy, and (c) Fracture toughness.

The results for fracture deformation shown in Figure 19(a) indicate that binders tested in the SENB at temperatures below their T_g show brittle behavior with fracture deformation/deflection consistently at or below 0.35 mm. The overall trend in the data show a clear differentiation between the brittle (below T_g) and ductile region (above the T_g) for all binders tested.

The ductile to brittle cut-off value is harder to discern when using fracture energy (G_f), which is influenced by both fracture load as well as the fracture deflection. Although 90% of the binders tested in the brittle temperatures fractured at energies at or below 10 J/m^2, a few binders in the ductile zone also fractured at energies below this value.

Figure 19(c) shows an overall increase of the fracture toughness (i.e., increase of fracture load as measured by K_{IC}) as the binder enters the brittle temperature zone. However, K_{IC} does not show the clear differentiation of this parameter around this transition region. It is therefore not recommended for estimation of the ductile-brittle transition.

Assuming binders fracturing at deflections below 0.35 mm are in fact exhibiting brittle behavior, one may compare the ability of the SENB and BBR systems to capture the brittle-ductile transition (Figure 20). It can be seen in Figure 20 that a large number of binders performing within the 300 MPa stiffness limit have fracture deflections well below the 0.35 mm limit discussed earlier, further highlighting the superior ability of using the SENB fracture deflection as an indication of the brittleness of the binder. It is envisioned that by controlling the binder SENB fracture energy and fracture deflection as performance and brittleness indicators respectively, one may better rank and discriminate wide ranges of binder sources and modification types, in comparison to current specifications.

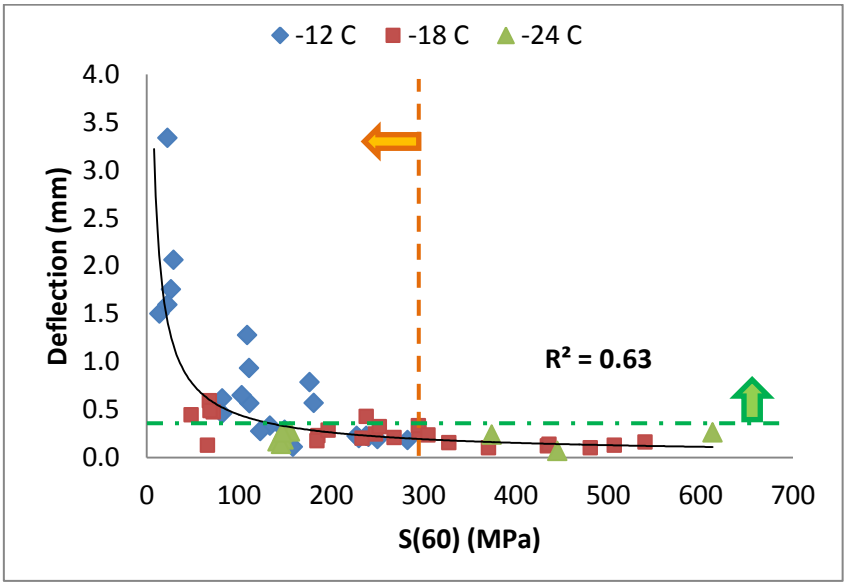

Figure 20. Comparison of SENB fracture deflection with BBR stiffness of modified and unmodified binders tested at -12, -18 and -24°C (orange line indicates BBR S(60) limit criteria and green line shows SENB deflection of 0.35mm).

The fracture deformation of 0.35 mm which appears to be a suitable ductile-brittle transition limit, as observed in Figure 19(a) is interestingly very similar to the suggested 0.30 mm deformation value for the T_{FT} parameter suggested by the CEN/TS 15963:2010 standard specification. In SENB testing, as the test temperature decreases, the fracture deformation decreases exponentially. The T_{FT} parameter is an indicator of the temperature at which the

binder goes through a brittle to ductile transition. Figure 21(a) shows an example of how T_{FT} is calculated based on deformation at fracture from three SENB tests. Figure 21(b) shows a good correlation between T_{FT} and T_g. This finding also indicates that the SENB can be used as possible surrogate test to estimate the T_g of binders. Estimation of the T_{FT} parameter based on fracture energy measurements instead of deformation at fracture was attempted and results are presented in Figure 22. It can be seen from Figures 21 and 22 that T_{FT} , estimated based on deformation at fracture, provides a better indication of the glass transition of the binders.

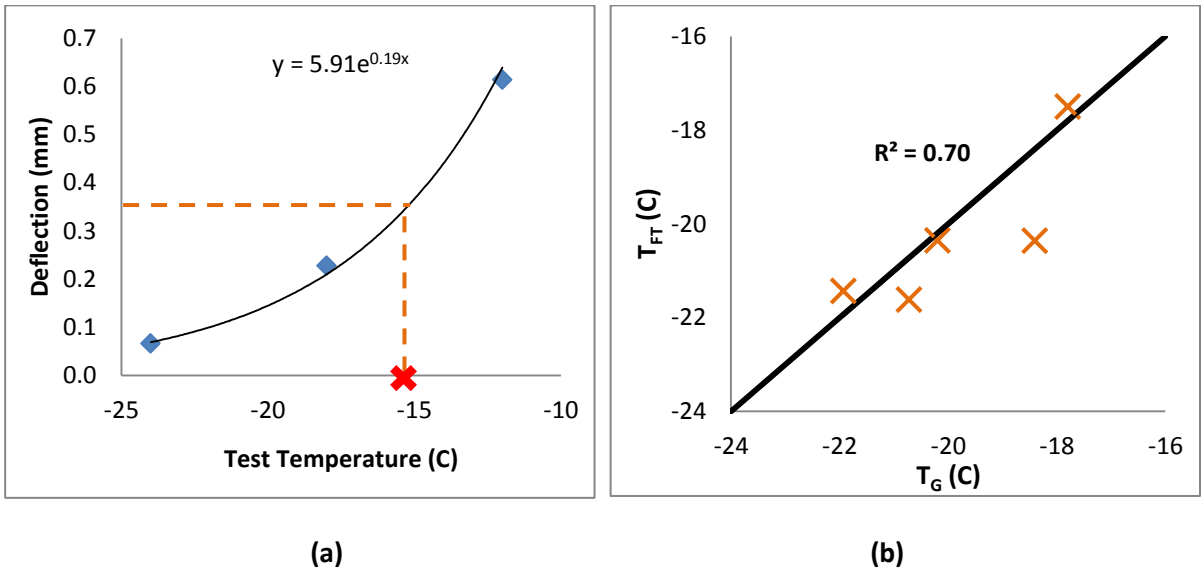

Figure 21. (a) Exponential curve fitting to fracture deflection at three test temperatures to use for calculation of T_{FT}, and (b) The Glass Transition Temperature (°C) Plotted against the T_{FT} (°C) Parameter from the SENB.

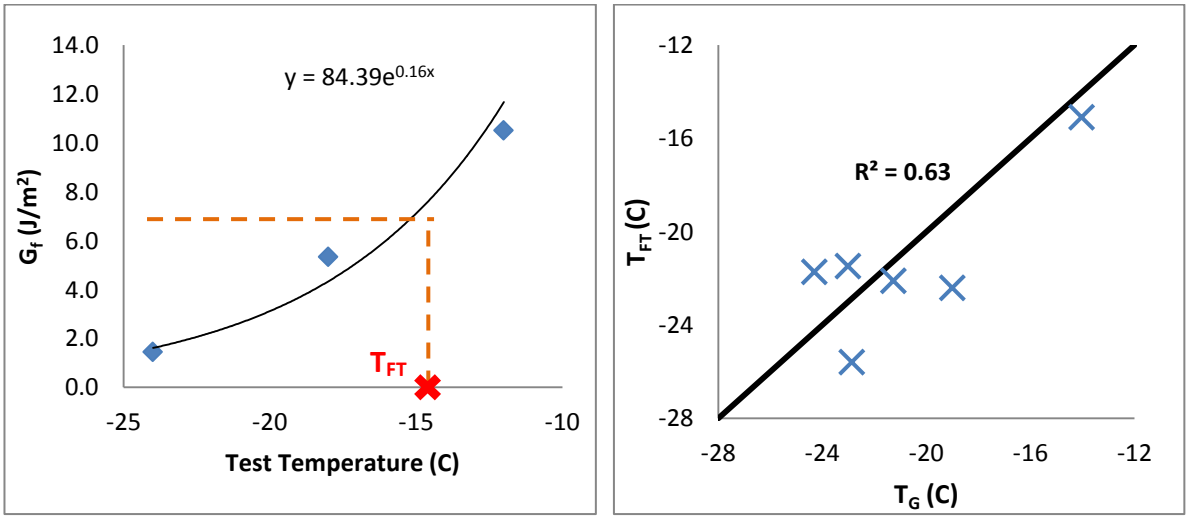

Figure 22. (a) Exponential curve fitting to fracture energy at three test temperatures to use for calculation of T_{FT}, and (b) The Glass Transition Temperature (°C) Plotted against the T_{FT} (°C) Parameter from the SENB.

Considering the relative ease of using the SENB compared to other binder fracture test procedures, it can be stated that the SENB fracture energy (G_f) and/or fracture deformation can be used to effectively differentiate binder low temperature performance and establish the binder brittle-ductile transition region. The test is a suitable alternative for the DTT to measure strain tolerance and to be used as a compliment to the current BBR specification.

Validation of SENB Measurements

Comparison of SENB Results to Mixture Fracture Tests

The relationship between binder and mixture fracture properties was also investigated by comparing results from SENB testing and mixture fracture properties obtained using the Semi Circular Bending (SCB) and the Disc Compact Tension (DCT) tests. Comparisons were made between the SENB tests done on binders from MnROAD cells and mixture SCB and DCT tests performed on samples from these cells by the University Minnesota and the University of Illinois at Urbana-Champaign. Figure 23 shows the correlations found for toughness (K_{IC}) and the fracture energy (G_f) of binders and mixes.

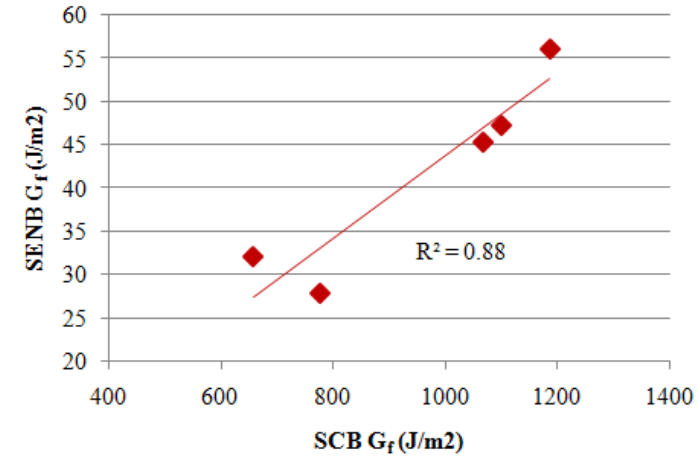

(a)

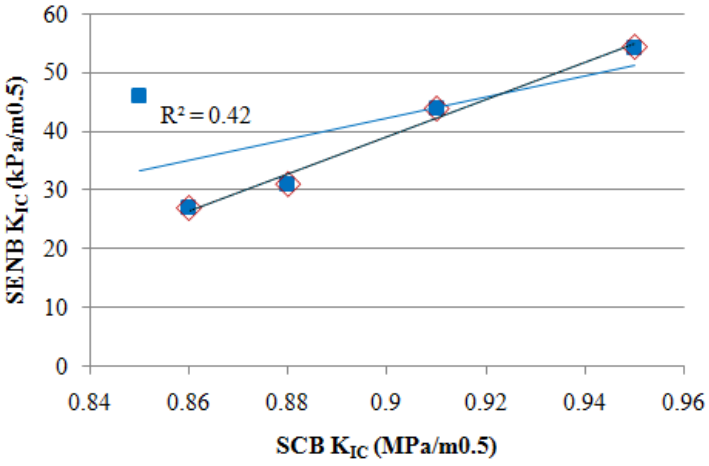

(b)

Figure 23. (a) SENB and SCB G_f compared (b) SENB and SCB K_{IC} compared

It was noted that one point in Figure 23(b) significantly decreased the correlation between binder and mixture data. It was later discovered that the mixture specimens for that specific cell had an unusually high deviation in air voids compared to the target air voids. Overall it is seen that a relatively good relationship between the SENB and the SCB results exists. Comparison of the test results between the SENB and the DCT did not yield any apparent correlation (plots not shown). This is thought to be due to the significantly higher loading rates in the DCT compared to the SCB and SENB, both which use a similar loading rate.

Comparison of SENB Results to LTPP Field Data

The newly developed SENB testing results was validated by using field performance information from the Long Term Pavement Performance (LTPP) program. Selected LTPP binders were tested with the SENB procedure and results were compared to field thermal cracking performance recorded in the LTPP database. This work was conducted as part of collaboration with the Asphalt Research Consortium (ARC) project.

The materials tested include binders with SHRP ID numbers designated in Table 3. All binders were subject to RTFO aging. Table 3 shows fracture energy (G_f) and fracture toughness (K_{IC}) of the LTPP binders measured at -12°C. Due to the different climatic conditions in the LTPP sections, it was decided to normalize the amount of cracking in each section to its corresponding Freeze Index (degree days below 0°C). Also, the ranking of the binders based on normalized field performance, PG grade, fracture energy, and fracture toughness is presented in Table 3. Based on the rankings shown, there seems to be a good relationship between the low temperature pavement performance and binder fracture energy. Generally, similar ranking for binders is observed for field performance and G_f. As shown in the table, when the sum of differences in ranking is determined, G_f gives the lowest sum of differences indicating that it is the best indicator to field cracks count as compared to PG grade or K_{IC}.

Table 3. SENB results at -12°C for LTPP binders.

SHRP ID	PG Grade	RANK Based on PG grade	No. of Transverse cracks per section/ Freeze Index ($\times 10^{-3}$)	RANK Based on Cracks count	G_f (J/m^2) (total)	RANK Based on G_f	K_{IC} (kPa.m$^{0.5}$)	RANK Based on K_{IC}
370901	64-22	4	702.58	7	5.45	7	26.83	6
370903	70-22	4	343.25	6	6.24	6	55.03	1
90961	58-34	2	9.26	4	44.2	2	31.98	5
90962	58-28	3	6.18	2	11.87	4	37.57	4
90903	64-22	4	24.71	5	10.98	5	38.54	3
89a902	52-40	1	7.01	3	103.82	1	23.12	7
350903	58-22	4	1	1	21.31	3	40.93	2
Sum of ranking difference= Sum of (Field Cracks – Other Rank)		14		0		8		16

Figure 24 show the relationship between fracture energy of the LTPP binders and normalized number of transverse cracks per section. The LTPP pavement sections with the highest normalized number of transverse cracks had relatively low binder fracture energy. The shape and trend of this curve is very similar to the curves previously reported in Phase I in which fracture properties of asphalt mixtures obtained with the Semi-Circular Bending Test (SCB) were compared to field performance measured in MnROAD sections. These results indicate the potential of using G_f as thermal cracking performance index for asphalt binders.

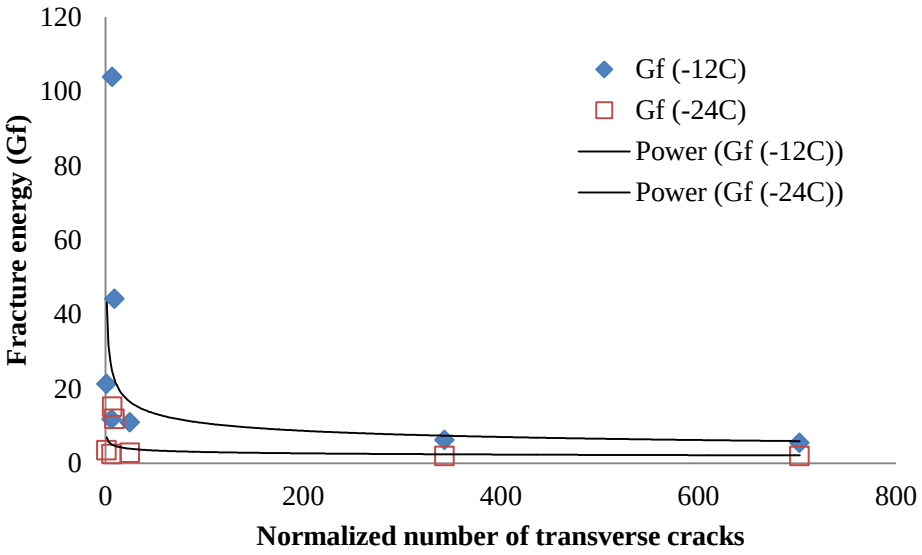

Figure 24. G_f vs. normalized number of transverse cracks at -12°C and -24°C.

The ability of the SENB load-deflection curve to clearly estimate the low temperature performance of the binders can be seen in Figure 25. The section ID and respective LTPP performance index for each curve are presented on the plots. It can be seen that a very wide range of change in fracture deflection and consequently in G_f exists between binders. The SENB test clearly discriminate among the various binder types in terms of low temperature performance.

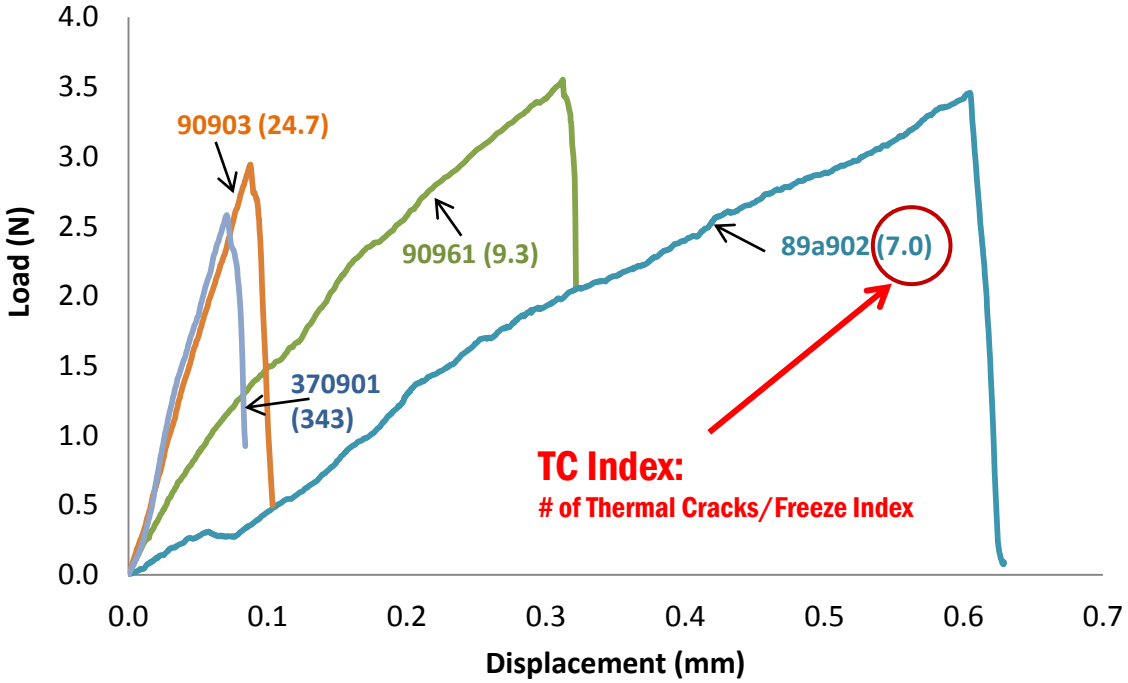

Figure 25. Comparison of SENB load-deflection curves for LTPP binders. Lower performance index shows better performance [Labels: LTPP code (Performance Index)]

Summary of Findings

The Single-Edge Notch Bending (SENB) test using beam samples made with the Bending Beam Rheometer (BBR) molds is a relatively simple test that can be carried out in a time frame similar to the current BBR test. The test was shown to be able to capture the ductile-brittle transition, which is a good indicator of the glass transition of the binder. Furthermore, in contrast to the BBR, it is believed that the BBR-SENB test can capture the non-linear and damage resistance behavior of binders at low temperatures. These unique properties make the BBR-SENB test a potentially ideal performance characterization test, as it allows for the estimation of the relaxation modulus and the fracture resistance properties of binders. It is recognized that stress buildup in pavements and cracking is a complex phenomenon that requires knowledge of multiple factors such as moduli, shrinkage rates, and resistance to fracture. The following detailed findings can be drawn from the development of the BBR-SENB and corresponding experimental results:

- Results collected with the BBR-SENB test clearly show that binders of same low temperature grade can have significantly different fracture energy (G_f) measured at the grade temperature. For example, binders graded as PG (xx-28) showed a range of 5 to 80 J/m^2 measured at -12°C.
- The results of the ABCD test do not correlate with the glass transition temperature nor with the fracture energy measured with the BBR-SENB.
- SENB experimental results showed that deformation at maximum load and fracture energy (G_f) are good indicators of the low temperature performance of asphalt binders in mixtures and pavements.
- The T_{FT} parameter (i.e., temperature at which deformation at fracture = 0.35 mm), calculated from SENB tests at multiple temperatures, is well correlated to the glass

transition temperature (T_g). These results indicate the potential of using the SENB test as an estimation method for the binder glass transition temperature.

- Fracture toughness (K_{IC}) cannot clearly differentiate the ductile to brittle transition binders. It is also not found to relate to performance of mixture in pavements, thus it is not recommended as performance indicator.
- Physical hardening can have significant effect on fracture behavior. The limited data collected with the SENB show that for some binders G_f values could decrease but for others it could increase by as much as 100% after 72 hours of isothermal conditioning.
- Validation efforts using LTPP materials indicate the potential of using SENB measurements to accurately estimate the role of binders in field thermal cracking performance. Results show that G_f can be used to rank binders according to field cracking significantly better than PG grade.

References

1. American Association of State Highway and Transportation Officials (AASHTO) Standard T313-05, "Standard method of test for determining the flexural creep stiffness of asphalt binder using the Bending Beam Rheometer (BBR)," Standard Specifications for Transportation Materials and Methods of Sampling and Testing, 25th Edition, 2005.

2. T. Hoare and S. Hesp, "Low-Temperature Fracture Testing of Asphalt Binders: Regular and Modified Systems." Transportation Research Record 1728, pp. 36-42, 2000.

3. S. Hesp, "An improved low-temperature asphalt binder specification method." Final report, NCHRP-IDEA contract 84 and Ministry of Transportation Ontario Contract 9015-A-000190, 2003.

4. E. Chailleux, and V. Mouillet, "Determination of the low temperature bitumen cracking properties: fracture mechanics principle applied to a three points bending test using a non-homogeneous geometry," ICAP Proceedings, Quebec, 2006.

5. E. Chailleux, V. Mouillet, L. Gaillet, D. Hamon, "Towards a Better Understanding of the Three Point Bending Test Performed on Bituminous Binders. Advanced Characterization of Pavement and Soil Engineering Materials." Taylor & Francis Group, ISBN 978-0-415-44882-6, 1075-1084, London, 2007.

6. ASTM Standard E399, "Standard Test Method for Linear-Elastic Plane-Strain Fracture Toughness K_{IC} of Metallic Materials", West Conshohocken, PA, 2006, DOI: 10.1520/E0399-09E01, www.astm.org.

7. Velasquez R., Tabatabaee, H.A. and Bahia, H.U., Low Temperature Cracking Characterization of Asphalt Binders by Means of the Single-Edge Notch Bending (SENB) Test. Journal of the Association of Asphalt Pavement Technologists, 2011.

8. ABAQUS, help documentation, ver. 6.6-1, 2006.

9. European Standard CEN/TS 15963:2010, "Bitumen and bituminous binders - Determination of the fracture toughness temperature by a three point bending test on a notched specimen," 2010.

10. Swiertz, D. Mahmoud, E., Bahia, H.U., Estimating the Effect of RAP and RAS on Fresh Binder Low Temperature Properties without Extraction & Recovery. Proceedings of the 90th Annual Meeting of the Transportation Research Board, Washington D.C, 2011.

11. S.S. Kim, "Direct Measurement of Asphalt Binder Thermal Cracking," Journal of Material in Civil Engineering. Volume 17, Issue 6, pp. 632-639, 2005.

12. Copeland, Reclaimed Asphalt Pavement in Asphalt Mixtures: State-of-the-Practice. FHWA Office of Infrastructure Research, 2009.

13. McDaniel, R. S., Soleymani, H., Anderson, R. M., Turner, P. and Peterson, R., Recommended use of Reclaimed Asphalt Pavement in the Superpave Mix Design Method. Web Document 30 (Project 9-12), NCHRP, 2000.

14. Bouldin, M., Dongre,, R., Rowe, G., Sharrock, M.J., Anderson, D. "Predicting Thermal Cracking of Pavements from Binder Properties-Theoretical Basis and Field Validation." Journal of the Association of Asphalt Pavement Technologists 69 (2000): 455.

15. Sushanta, R. and Hesp, S. "Low-Temperature Binder Specification Development: Thermal Stress Restrained Specimen Testing of Asphalt Binders and Mixtures." Transportation Research Record: Journal of the Transportation Research Board 1766, (2001): 7-14.